DOI: 10.15669/pnst.5.33

Progress in Nuclear Science and Technology
Volume 5 (2018) pp. 33-36

ARTICLE

Surface characterization of $(U,Nd)O_2$: the influence of trivalent-dopant on structure of UO_2

Jeongmook Lee[a*], Jandee Kim[a], Young-Sang Youn[a], Jong-Yun Kim[a,b] and Sang Ho Lim[a,b]

[a]*Nuclear Chemistry Research Division, Korea Atomic Energy Research Institute, 989-111 Daedeok-daero, Yuseong-gu, Daejeon, 34057, Republic of Korea;* [b]*Department of Radiochemistry & Nonproliferation, University of Science and Technology, 217 Gajeong-ro, Yuseong-gu, Daejeon, 34113, Republic of Korea*

The surface structures of $(U,Nd)O_2$ pellets were characterized by using Raman spectroscopy to study the influence of trivalent-dopant on a UO_2 surface lattice. The stoichiometry of each sample pellet was confirmed by analyzing the lattice parameter calculated from X-ray diffraction spectra. Raman spectra of the sample pellets showed the defect structures related to oxygen vacancies. The concentration of oxygen vacancies in $(U,Nd)O_2$ pellets is affected by the Nd doping level.

Keywords: uranium dioxide; neodymium doping; X-ray diffraction; Raman spectroscopy; oxygen vacancy; surface structure

1. Introduction

In the spent nuclear fuel (SNF) of a PWR, several actinide (An) and lanthanide (Ln) elements were dissolved in a UO_2 matrix like $(U,An)O_2$ or $(U,Ln)O_2$ solid solutions [1-4]. Those elements have affected the physical and chemical characteristic of SNF such as the structural change of fuel surface and the chemical states of uranium. For example, the structural activation site on the surface of SNF can strongly induce its corrosion or chemical reaction with ground water under a failure of the barrier [2]. It is thus important to identify the surface characteristics of SNF to understand the related surface reaction of SNF. There have been many efforts to characterize the influence of several elements on the surface structure of UO_2 using simulated fuels systemically [5-10]. These efforts are very helpful to understand the surface structural properties of SNF.

In this paper, $(U,Nd)O_2$ as a simple simulated fuel has been investigated using X-ray diffraction and Raman spectroscopy to understand the influence of a trivalent-dopant on the surface structure of UO_2. Nd is a major trivalent element formed in spent nuclear fuel [11,12]. The effect of Nd-doping on the UO_2 structure was analyzed and compared with previous published studies. This study aims to provide important implications for interpretation of defect structure caused by trivalent doping in uranium dioxide.

2. Experimental Section

UO_2 and Nd_2O_3 powders were used as starting materials. The calculated amount of both powders for UO_2, $U_{0.99}Nd_{0.01}O_{2-x}$ and $U_{0.95}Nd_{0.05}O_{2-x}$ were ground and mixed in an agate mortar. The powder mixtures were compacted to a round pellet with ~ 1 mm thickness. The pellets were sintered under a reducing condition with flowing hydrogen at 1700 ℃ for 18 h and followed by annealing under the same condition at 1200 ℃ for 12 h. The sintered pellets were placed in a vacuum container to prevent surface oxidation.

UO_2 and $U_{1-y}Nd_yO_{2-x}$ pellets were characterized by X-ray diffraction (XRD) using a Bruker AXS D8 Advance Xray Diffractometer with CuKa radiation. XRD data were collected within the range of 20 to 120°. The lattice parameters were calculated through the Pawley refinement process using the TOPAS software (Version 4.2) of Bruker.

Raman spectroscopy was also applied to measure the surface structure of the sample pellets with an ANDOR Shamrock SR500i spectrometer. The laser with a wavelength of 632.8 nm from a He-Ne laser was focused onto the sample through a 50-fold magnification lens in an Olympus microscope. Raman spectra were measured at five different positions on the surface over the range 400 ~ 1200 cm^{-1} with an exposure time of 100 s.

3. Results and discussion

The lattice parameters of all sample pellets refined from their XRD spectra are shown as black square dots in **Figure 1**. Those values linearly decrease as the Nd doping level increses. This lienar relationship was well-matched with the case of $U_{1-y}Nd_yO_{2-y/2}$ type rather than that of $U_{1-y}Nd_yO_2$ type [13]. The analysis of

*Corresponding author. Email: leejm@kaeri.re.kr

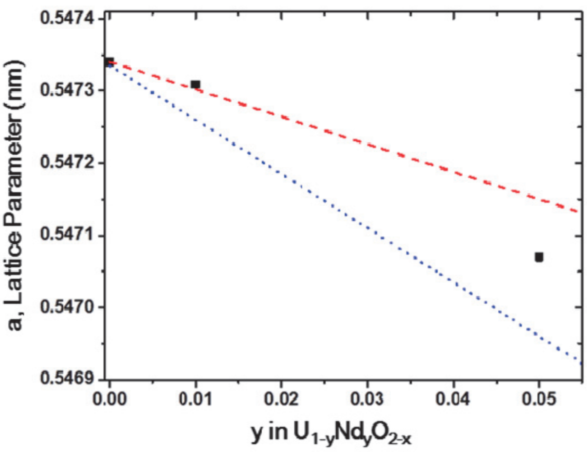

Figure 1. The lattice parameter of UO_2 and $U_{1-y}Nd_yO_{2-x}$ pellets are denoted as the Nd content changes. Red dashed and blue dotted lines represent the linear relationships for $U_{1-y}Nd_yO_{2-y/2}$ and $U_{1-y}Nd_yO_2$ types, respectively, with increasing Nd content [13].

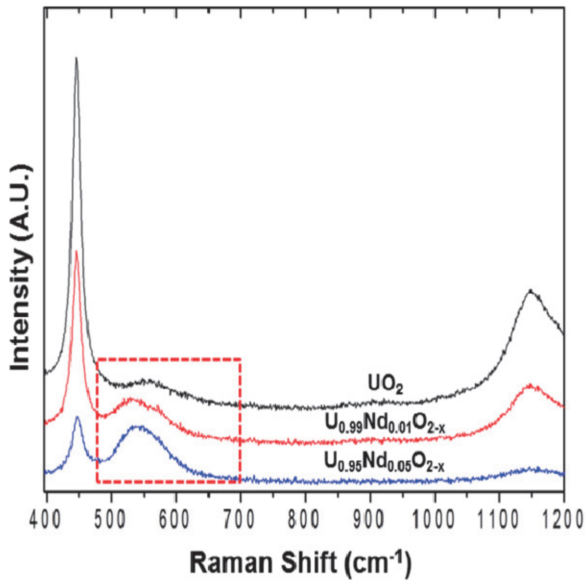

Figure 2. Raman spectra of UO_2, $U_{0.99}Nd_{0.01}O_{2-x}$ and $U_{0.95}Nd_{0.05}O_{2-x}$ pellets from top to bottom. Red dashed box indicates the defect structure of $U_{0.99}Nd_{0.01}O_{2-x}$ and $U_{0.95}Nd_{0.05}O_{2-x}$ pellets.

the lattice parameter indicated that the manufactured pellets in this study have hypo-stoichimetric form. The $U_{0.95}Nd_{0.05}O_{2-x}$ pellet, however, was somewhat deviated from the $U_{1-y}Nd_yO_{2-y/2}$ type to $U_{1-y}Nd_yO_2$ type. This deviation might be from a lack of reducing power during sintering for higher doping contents.

Raman spectra of the UO_2, $U_{0.99}Nd_{0.01}O_{2-x}$ and $U_{0.95}Nd_{0.05}O_{2-x}$ pellets are shown in Figure 2. These are the averaged spectra from five different positions on the surface of the pellets. The intensity of the peak at ~ 445 cm^{-1} assigned as the U-O symmetric stretching (T_{2g} mode) of the UO_2 fluorite struecture [14-16] and that of the broad peak at ~ 1150 cm^{-1} representing quasi-perfect fluorite structure of UO_2 [17,18] distinctly decrease with the increase in Nd content. On the other hand, the intensity of the broad band between 500 and 700 cm^{-1} dramatically inceases with increasing Nd concentration. These distinct featrues have been ascribed to the UO_2 lattice distortion due to the existence of defect structures or lattice damage [5-10,18].

To thoroughly interpret the lattice distorsion of $U_{1-y}Nd_yO_{2-x}$ pellets, the Raman spectra in **Figure 2** were analyzed in detail. Raman spectra for $U_{0.99}Nd_{0.01}O_{2-x}$ and $U_{0.95}Nd_{0.05}O_{2-x}$ pellets between 400 and 700 cm^{-1} were deconvluted into four Lorentzian peaks at ~ 445, ~535, ~575 and ~630 cm^{-1} as shown in **Figure 3**. The peak at ~535 cm^{-1} has been attributed to the oxygen vacancies [5-9]. This peak was also interpreted as a local phonon mode associated with an oxygen-vacancy-induced lattice distortion [5] and observed in the Raman spectra of Gd-, Dy-doped UO_2 [6], $U_{1-y}La_yO_{2-y/2}$ [7], and $(U,Am)O_{2-\delta}$ [8], $U_{1-y}Gd_yO_{2-x}$ [9] samples. The important point is that the peak ralated the oxygen vacancies is only observed in trivalent-doping UO_2 and not tetravalent-doping UO_2 like $(U,Th)O_2$ [10]. For trivalent-doping UO_2, the 3+ oxidation state of trivalent-dopant substituted for U(IV) in UO_2 lattice can make oxygen vacancies to preserve electroneutrality in $U^{4+}{}_{1-x-y}U^{5+}{}_xM^{3+}{}_yO^{2-}{}_{2+x/2-y/2}$. However,

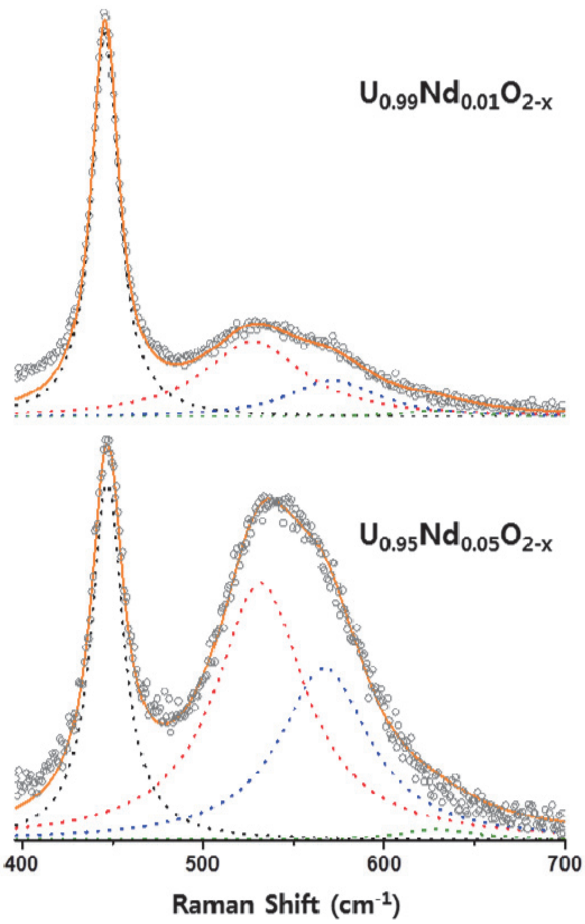

Figure 3. Deconvoluted Raman spectra of $U_{0.99}Nd_{0.01}O_{2-x}$ (up) and $U_{0.95}Nd_{0.05}O_{2-x}$ (bottom) pellets with Lorentzian peaks at ~ 445, ~535, ~575 and ~630 cm^{-1}. Open circles and orange continuous line indicate the experimental data and fitted line using Lorentzian peaks, respectively.

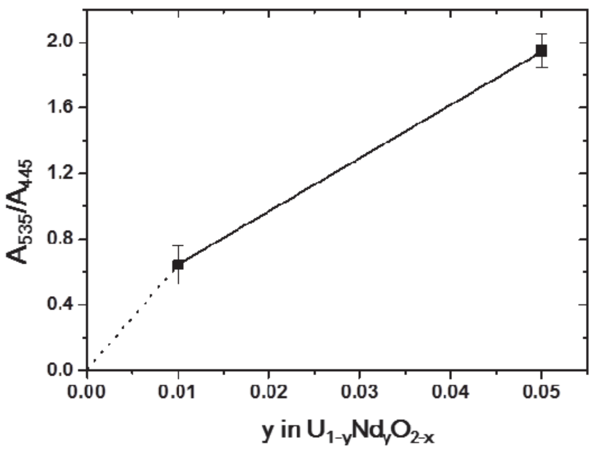

Figure 4. The area ratio between peaks at ~535 and ~445 cm^{-1} as a function of Nd content in $U_{1-y}Nd_yO_{2-x}$ pellets.

there is less chance to create oxygen vacancies for $U^{4+}{}_{1-y}M^{4+}{}_yO^{2-}{}_2$ in which U(IV) was simply replaced with stable M(IV). This interpretation could expect that the oxygen vacancy concentration increases as the doping level increases. **Figure 4** shows that the area ratio between peaks at ~535 and ~445 cm^{-1}, representing the relative concentration of oxygen vacancies in the UO_2 fluorite lattice structure, increases with Nd doping level. A similar feature was also observed in the case of $U_{1-y}La_yO_{2-y/2}$ [7], and $U_{1-y}Gd_yO_{2-x}$ [9] samples. These results fully support that the influence of trivalent-dopant on the structure of UO_2 is the creation of an oxygen vacancy and its concentration is systemically related to the trivalent-doping level. The peak at 540 cm^{-1} in the Raman spectrum of SIMFUEL [6], attributed to the oxygen vacancies, could be strongly induced from the influence of trivalent-dopants in the UO_2 lattice.

The peak at ~575 cm^{-1} has been attributed to a first-order longitudinal optical (L-O) phonon mode [17,18]. Although this mode is originally forbbiden in the perfect fluorite structure of UO_2, it is allowed under the break down of selection rule from low symmetry due to a crystal lattice disorder [17]. The oxygen vacancies in $U_{1-y}Nd_yO_{2-x}$ pellets could induce a lattice disorder, and thus first-order L-O Raman modes are allowed, as shown in Figure 3.

The peak ascribed to the presence of U_4O_9 due to surface oxidtion was rarely observed at ~630 cm^{-1} [19]. This confirms a marginal surface oxidation of $U_{0.99}Nd_{0.01}O_{2-x}$ and $U_{0.95}Nd_{0.05}O_{2-x}$ pellets.

4. Conclusion

To characterize the influence of trivalent-dopant on the surface structure of UO_2, the surface of $U_{1-y}Nd_yO_{2-x}$ pellets was analyzed using XRD and Raman spectroscopy techniques. The lattice parameters calculated from XRD spectra confirm the hypo-stoichiometric form of $U_{1-y}Nd_yO_{2-x}$. Raman spectra of $U_{0.99}Nd_{0.01}O_{2-x}$ and $U_{0.95}Nd_{0.05}O_{2-x}$ pellets show the creation of the oxygen vacancies on the surface lattice and the increasing oxygen vacancy concentration with increasing Nd doping level. These results combined with published literature confirm that trivalent-dopants including Nd strongly affect the surface structure of UO_2 with oxygen vacancies created owing to a charge compensation. The characterization of $(U,Nd)O_{2-x}$ surface structures can provide important implications for characterizing the surface of SNF.

Acknowledgements

This work was supported by the National Research Foundation of Korea (NRF) grant funded by the Korean government (MSIT) (2017M2A8A5014754)

References

[1] H. Kleykamp, The chemical state of the fission products in oxide fuels, *J. Nucl. Mater.* 131 (1985), pp. 221-246.

[2] R.J.M. Konings, T. Wiss and O. Beneš, Predicting material release during a nuclear reactor accident, *Nat. Mater.* 14 (2015), pp. 247-252.

[3] R.C. Ewing, Long-term storage of spent nuclear fuel, *Nat. Mater.* 14 (2015), pp. 252-257.

[4] J. Bruno and R.C. Ewing, Spent nuclear fuel, *Elements* 2 (2006), pp. 343-349.

[5] L. Desgranges, Y. Pontillon, P. Matheron, M. Marcet, P. Simon, G. Guimbretière and F. Porcher, Miscibility gap in the U−Nd−O phase diagram : a new approach of nuclear oxides in the environment?, *Inorg. Chem.* 51 (2012), pp. 9147-9149.

[6] M. Razdan and D.W. Shoesmith, Influence of trivalent-dopants on the structural and electrochemical properties of uranium dioxide (UO_2), *J. Electrochem. Soc.* 161 (2013), pp. H105-H113.

[7] Z. Talip, T. Wiss, P.E. Raison, J. Paillier, D. Manara, J. Somers and R.J.M. Konings, Raman and X-ray studies of uranium-lanthanum-mixed oxides before and after air oxidation, *J. Am. Ceram. Soc.* 98 (2015), pp. 2278-2285.

[8] F. Lebreton, D. Horlait, R. Caraballo, P.M. Martin, A.C. Scheinost, A. Rossberg, C. Jégou and T. Delahaye, Peculiar behavior of $(U,Am)O_{2-\delta}$ compounds for high americium contents evidenced by XRD, XAS, and Raman spectroscopy, *Inorg. Chem.* 54 (2015), pp. 9749-60.

[9] J. Lee, J. Kim, Y.-S Youn, N. Liu, J.-G. Kim, Y.-K. Ha, D.W. Shoesmith and J.-Y. Kim, Raman study on structure of $U_{1-y}Gd_yO_{2-x}$ (y=0.005, 0.01, 0.03, 0.05 and 0.1) solid solutions, *J. Nucl. Mater.* 486 (2017), pp. 216-221.

[10] R. Rao, R.K. Bhagat, N.P. Salke and A. Kumar, Raman spectroscopic investigation of thorium dioxide-uranium dioxide (ThO_2-UO_2) fuel materials, *Appl. Spectrosc.* 68 (2014), pp. 44-48.

[11] D. Serrano-Purroy, F. Clarens, E. González-Robles,

J.P. Glatz, D.H. Wegen, J. de Pablo, I. Casas, J. Giménez and A. Martínez-Esparza, Instant release fraction and matrix release of high burn-up UO_2 spent nuclear fuel: effect of high burn-up structure and leaching solution composition, *J. Nucl. Mater.* 427 (2012), pp. 249-258.

[12] E. González-Robles, D. Serrano-Purroy, R. Sureda, I. Casas and J. de Pablo, Dissolution experiments of commercial PWR (52 MWd/kgU) and BWR (53 MWd/kgU) spent nuclear fuel cladded segments in bicarbonate water under oxidizing conditions. Experimental determination of matrix and instant release fraction, *J. Nucl. Mater.* 465 (2015), pp. 63-70.

[13] T. Ohmichi, S. Fukushima, A. Maeda and H. Watanabe, On the relation between lattice parameter and o/m ratio for uranium dioxide-trivalent rare earth oxide solid solution, *J. Nucl. Mater.* 102 (1981), pp. 40-46.

[14] G.C. Allen and I.S. Butler, Characterisation of uranium oxides by micro-Raman spectroscopy, *J. Nucl. Mater.* 144 (1987), pp. 17–19.

[15] P.R. Graves, Raman microprobe spectroscopy of uranium dioxide single crystals and ion implanted polycrystals, *Appl. Spectrosc.* 44 (1990), pp. 1665-1667.

[16] G.M. Begun, R.G. Haire, W.R. Wilmarth and J.R. Peterson, Raman spectra of some actinide dioxides and of EuF_2, *J. Less Common Met.* 162 (1990), pp. 129-133.

[17] T. Livneh and E. Sterer, Effect of pressure on the resonant multiphonon Raman scattering in UO_2, *Phys. Rev. B.* 73 (2006), p. 085118.

[18] H. He and D. Shoesmith, Raman spectroscopic studies of defect structures and phase transition in hyper-stoichiometric $UO_{(2+x)}$, *Phys. Chem. Chem. Phys.* 12 (2010), pp. 8108-8117.

[19] L. Desgranges, G. Baldinozzi, P. Simon, G. Guimbretière, and A. Canizares, Raman spectrum of U_4O_9: a new interpretation of damage lines in UO_2, *J. Raman Spectrosc.* 43 (2012), pp. 455-458.